Brass Corrosion under a single droplet of NaCl

G A. EL-Mahdy[*], Amro K.F. Dyab, Ayman M. Atta , Hamad A. Al-Lohedan

King Saud University, Chemistry Department, College of Science, P.O.Box - 2455, Riyadh - 11451, Saudi Arabia
[*]E-mail: gamalmah2000@yahoo.com

A droplet of NaCl was gently placed horizontally on brass surface and corrosion rate, contact angle, volume loss and droplet height were monitored with droplet holding time. The corrosion rate of brass decreases during the initial stage of monitoring then slowly increases and eventually attains a steady state value during the last stage of monitoring. The droplet height continually dropped during the evaporation process, while the volume loss increases as the droplet holding time increases. The drop diameter remained relatively constant, while the contact angle continually decreased as droplet holding time progressed. A mechanism describing the successive stages of brass corrosion is proposed.

1. INTRODUCTION

Copper and its alloys are widely used in many industrial fields, especially in marine applications, external constructions as roofs, facades and claddings. The superior properties of copper and its alloys may be attributed to beneficial physical, mechanical and corrosion resistance properties. Brass has various industrial applications and economic importance due to resistance against corrosion. The corrosion behavior of brass with respect to dezincification, de-alloying, and stress corrosion has been studied. Dezincification is a known as de-alloying process that designates a loss of brass as an important physical/ mechanical characteristic resulting in surface destruction [1–7]. It was reported previously that ions as thiozionates, bromides, and iodides did not participate in dezincification process, while chlorides and sulphates enhanced dezincification process [1–5, 8]. It is well established that chloride [9-10] ions are considered as strong promoters of SCC of brass in the service environments. The passivation and localized corrosion of α and β – brass immersed in a buffer chloride solution has been studied by using X-ray Photo-electron, Auger Electron Spectroscopy and

Voltametry [11-13]. The Passivation of brass was attributed to the formation of a complex passive layer consisting of ZnO and Cu_2O. The anodic dissolution of β – brass was investigated by using chronoamperometry in Na_2SO_4, NaCl and H_2SO_4 solutions at 30 ^{o}C [14]. Although many studies on copper alloys and brasses, have been published [15-21], there has no been study focused on corrosion process under a single droplet of NaCl electrolyte. A number of complex and simultaneous interactions are triggered when a droplet impinges on a metal surface, such as precipitation of corrosion products and dissolution of the native surface oxides and development of pH, 22-23]. The influence of thickness of the electrolyte layer on the corrosion rate has been investigated by many researchers [24-36]. The aim of work is to investigate the corrosion process under a single droplet of NaCl. The work will be achieved by monitoring the corrosion rate, contact angle, droplet height as well as the volume loss of NaCl. A mechanism describing the successive stages of the corrosion process during the evaporation of the droplet is proposed.

2. EXPERIMENTAL PROCEDURE

2.1. Material and electrode preparation

Two-electrode cell configuration was fabricated from brass sheet with a composition of Cu 70% and Zn 30%. The electrode-cell, with dimensions of 0.1 mm (width) and 5 mm (length) was placed 0.1 mm apart, in an epoxy resin. The cell was placed horizontally facing upward, in an acrylic vessel. The electrode was abraded mechanically with SiC paper with differing grades of up to # 2000 mesh, and then cleaned with ethanol in an ultrasonic bath.

2.2 Electrochemical impedance spectroscopy (EIS)

The impedance measurement was conducted at 10 kHz and 10 mHz, using multichannel Solartron system 1470E. The polarization resistance (Rp) was determined by subtracting the high frequency impedance at 10 kHz from the low frequency impedance at 10 mHz.

2.3. Monitoring the droplet characteristics

The variations in contact angle, droplet height and volume loss and during the progress of corrosion process will be monitored using a drop shape analysis system (DSA-100, Kruss, Germany) with analysis software DSA4 software (V.1.0-03).

2.3. Corrosion products Morphology

The morphology of the corrosion products was examined by utilizing optical microscopy (Olympus BX-53) fitted with DP72 digital camera). Images were processed using Olympus CellSens v1.6.

3. RESULTS AND DISCUSSION

3.1. Monitoring volume loss and droplet height

Droplet shape at zero time
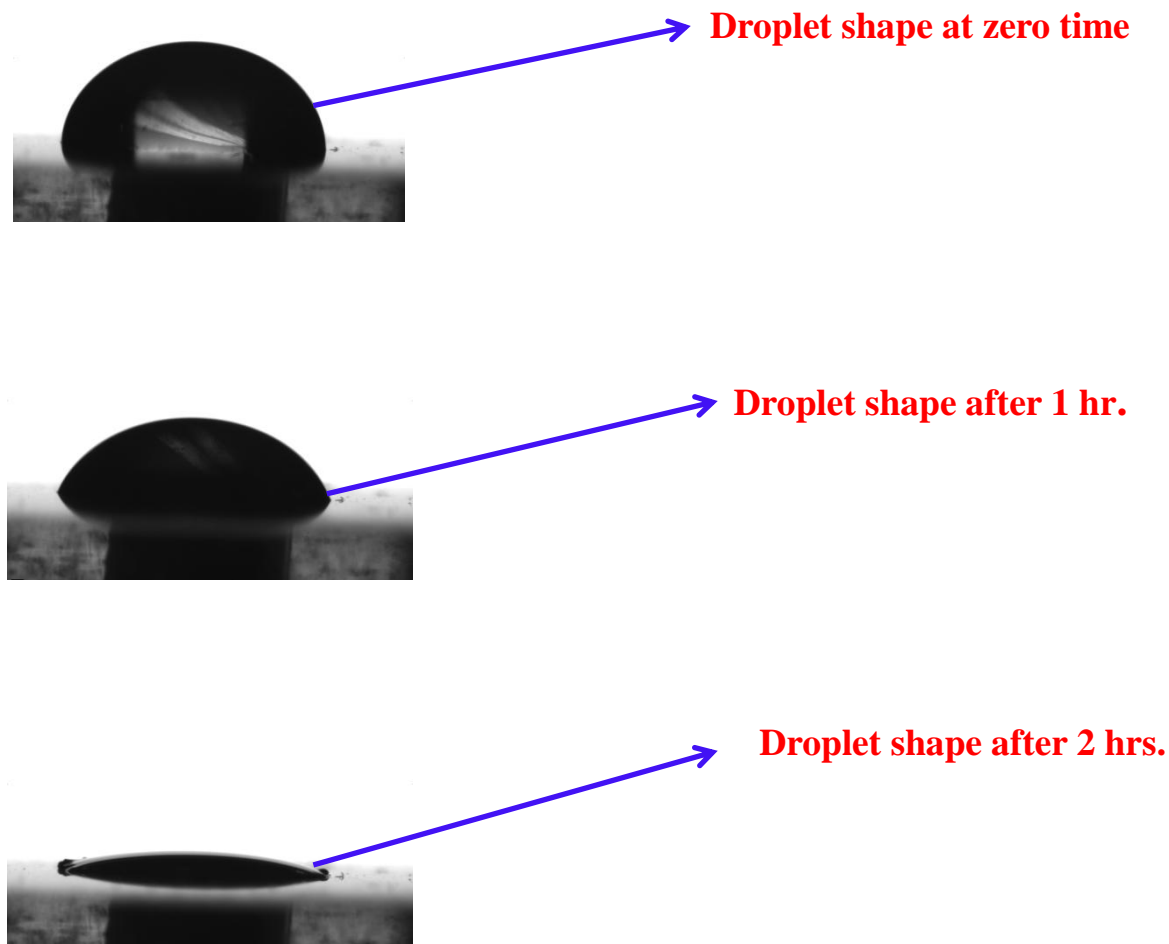
Droplet shape after 1 hr.

Droplet shape after 2 hrs.

Figure 1. Droplet shape at different holding times.

Fig.1 shows the droplet shape at different holding times. The rate of evaporation is depending on the difference between the vapor mass fraction at the droplet surface and the vapor mass fraction in the free stream. The lower the vapor mass fraction at the droplet surfaces the higher the rate of evaporation. The continuous increase in the volume loss with time shown in Fig. 2 can be attributed to an increase in the vapor mass fraction of the air surrounding the droplet. In addition, the result can be explained on the basis of an increase in the evaporation rate with time, which in turn accompanied by increasing the volume loss. The rate of droplet vaporization depends upon the nature of the evaporating liquid and upon the heat transferred to the liquid droplets after placing on the surface. The height of the droplets decreases nearly uniformly during the evaporation process as shown from the

data presented in Fig. 3. The decrease in height droplet could be attributed to an increase in evaporation rate with time. The droplet height is corresponding to the electrolyte thickness.
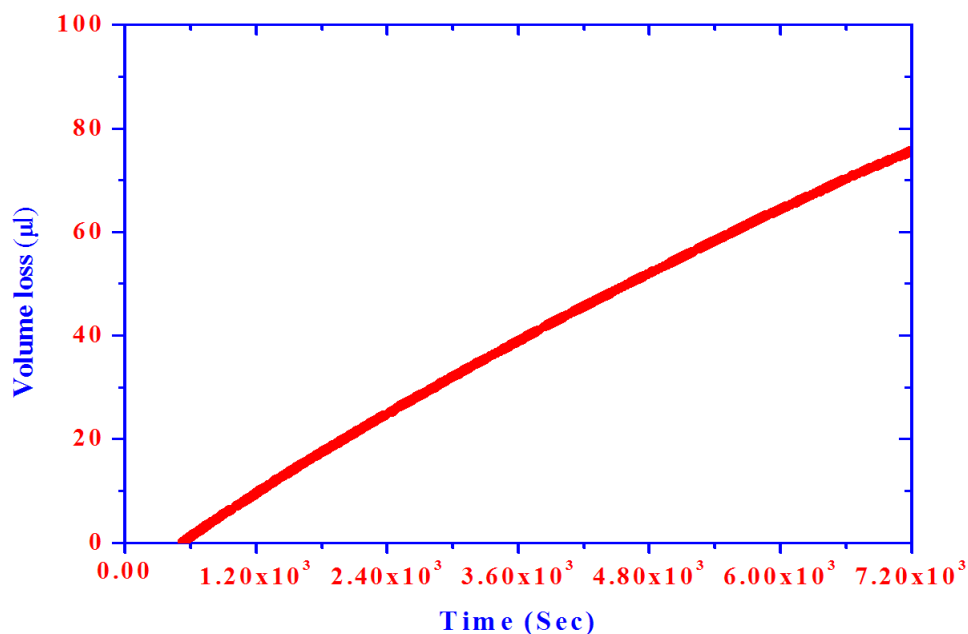

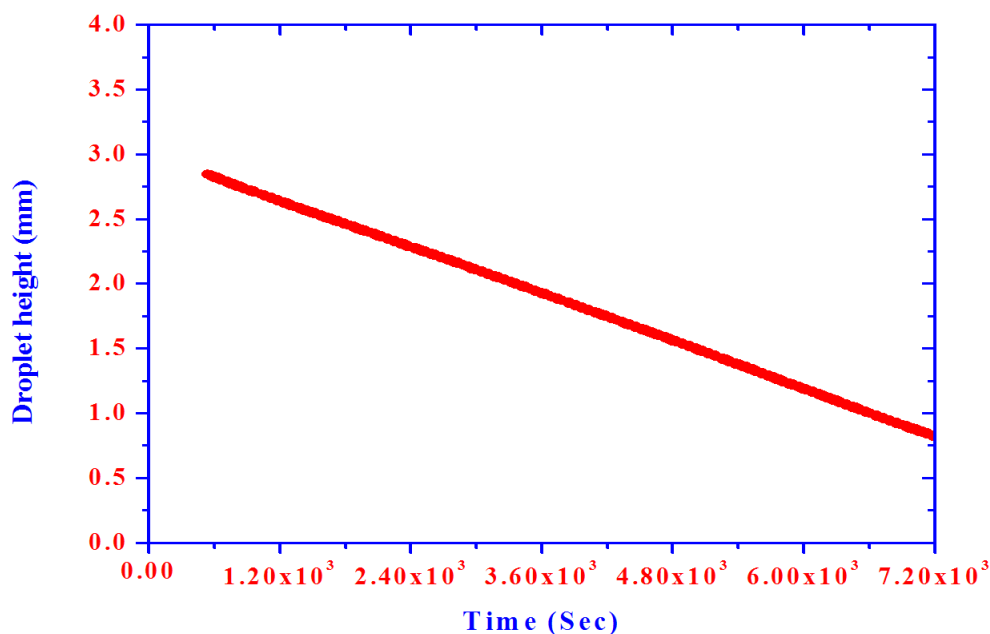**Figure 2.** Changes of volume loss with holding time.

Figure 3. Variation of droplet height (1/Rp) with time

It was established previously that the corrosion rate is mainly controlled by oxygen reduction under thin electrolyte layers [25]. The droplet shrinkage observed during the last stage of monitoring

may be attributed to an increase in capillary forces within the drop that would cause the droplet to experience a greater tendency to shrink during the last stage of evaporation process.

3.2 Monitoring the corrosion rate

Figure 4 shows the reciprocal of polarization resistance versus the exposure time measured after placing a single droplet of 0.5 M NaCl on the brass surface. The reciprocal of polarization resistance is proportional to the corrosion rate [37] as:

$$\text{Corrosion rate} = K / Rp \qquad (1)$$

$$K = ba.ba / 2.303(ba + bc) \qquad (2)$$

where ba and bc represent anodic and cathodic Tafel slope, respectively. The value of K is a function of metal and electrolyte [25, 31, 38] and can be assumed to be constant for a given metal/electrolyte system. The aggressive attack of chloride ion is remarkable on the corrosion rate of brass especially during the initial stage of monitoring, then slowly increases and eventually attains a steady state value during the last stage of monitoring.
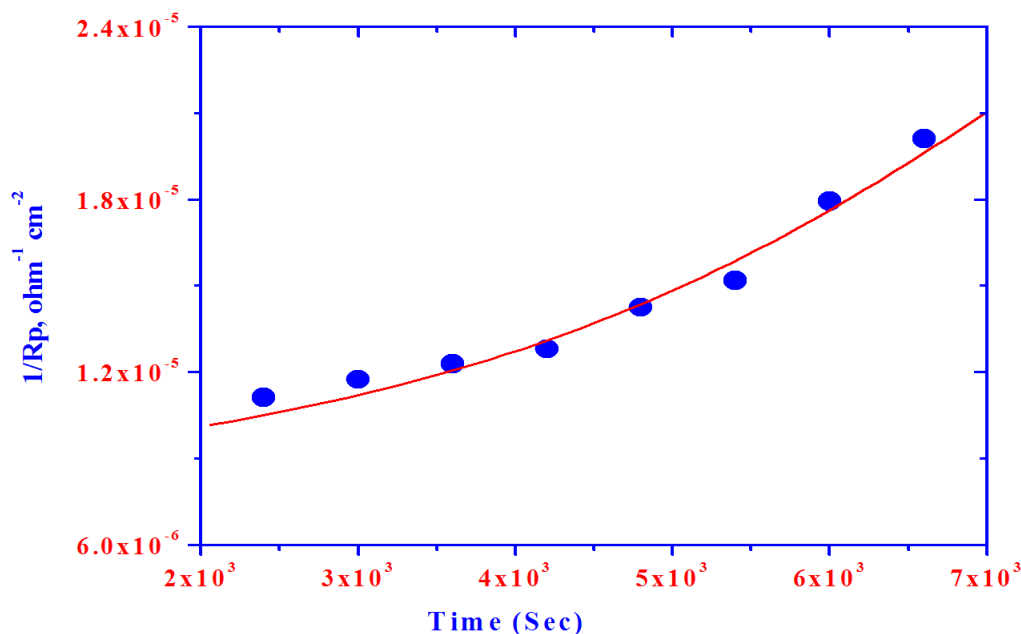

Figure 4. Variation of reciprocal of polarization resistance (1/Rp) with time.

The high corrosion rate observed during the initial stage was attributed to the continuous dissolution of the zinc. The rapid increase in corrosion rate was attributed to the dissolution of air-formed oxide film followed by brass dissolution . The gradual increase in corrosion rate experienced during the middle stage was attributed to the continuous dissolution of zinc and subsequent formation of the corrosion products as time progresses. The steady state observed during the last stages of exposure was attributed to the formation of stable corrosion products, which cover the entire surface of

brass. It was established previously from our investigation of brass in NaCl solution under wet-dry cyclic condition that Cu_2O, Cu, $Cu_2Cl(OH)_3$, $Zn_5(OH)_8Cl_2H_2O$ and ZnO were identified as corrosion products using X-ray diffraction (39) . It is clear that as droplet height decreases the corrosion rate increases as evident from correlation of the corrosion rate data shown in Fig. 4. with droplet height monitoring data shown in Fig. 3. The higher corrosion rate experienced at the lower the droplet height can be explained by a more reduction of oxygen resulting from high diffusion rate of oxygen through a shorter path as droplet height decreases.

3.3 Contact angle measurement

The droplet was gently placed horizontally on the surface facing upwards and the contact angle was monitored with holding time and the data is shown in Fig.5 The contact angle decreases with holding time and the measurement continued until before complete drying of the surface at which contact angle of the droplet began to oscillate and the measurements were terminated.
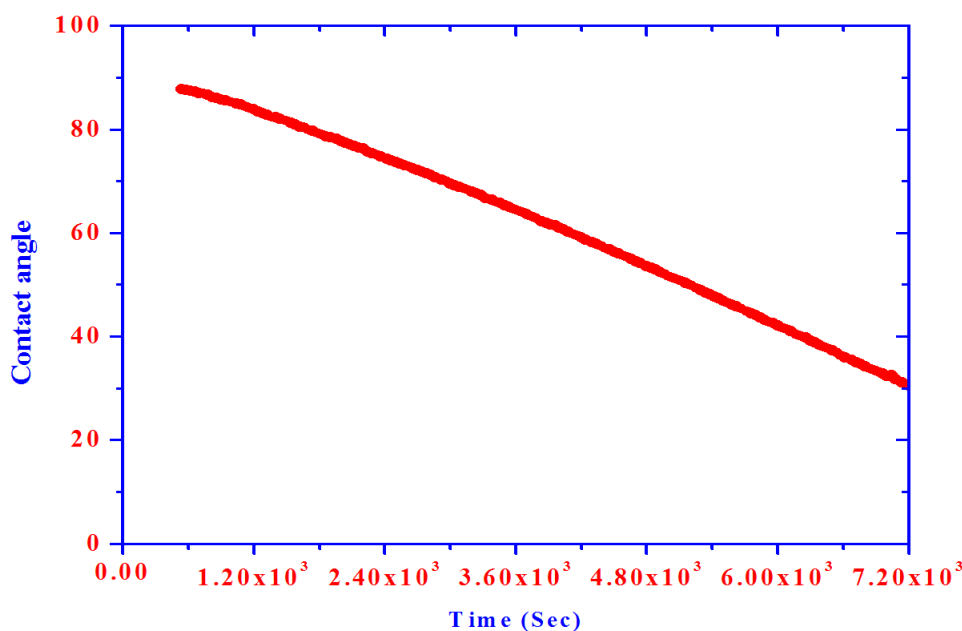

Figure 5. Dependence of contact angle on holding time.

Hence, the morphology showed that the droplet remained spherical-shaped throughout its lifetime. Fig. 6 shows the morphology of the droplet after complete drying, which indicated that the droplet remained spherical-shaped throughout its lifetime. This constancy of the droplet circular shape can be attributed to very low motion of the liquid within the droplet as well as the low spreading of the droplet on the surface. Fig. 7 shows the distributions of the corrosion products after complete drying of the droplet.
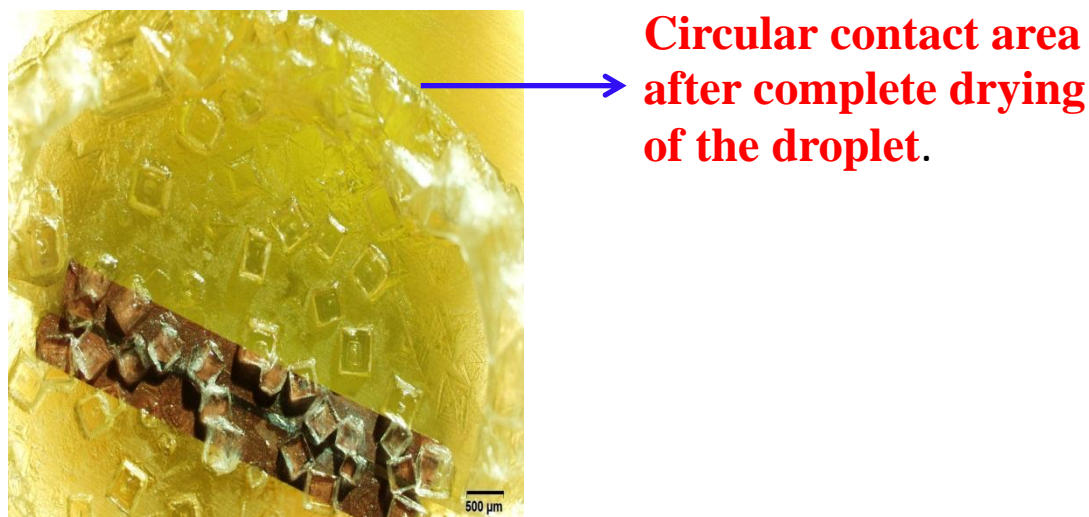
Figure 6. Photomicrograph representing the circular contact area after complete drying of the droplet
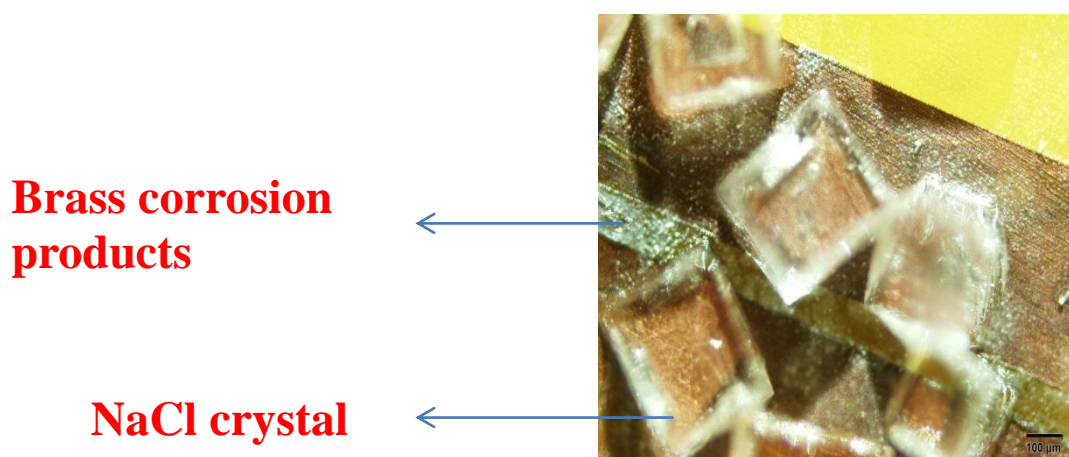

Figure 7. Photomicrograph representing the distributions of the corrosion products on the brass surface after complete drying of the droplet.

3.4. Mechanism of Brass corrosion within NaCl droplet

The corrosion of brass under a single droplet of NaCl can be described by dissolution/precipitation mechanism, which can be comprised in three stages as shown in Fig. 8. The higher corrosion rate experienced during the initial stages of brass holding the droplet can be attributed to the dissolution of the air -formed oxide film followed by underlying surface dissolution. Zinc dissolved preferentially and released faster than copper due to dezincification, which is accompanied by enrichment of brass surface with copper. The dissolution process of zinc can be described as:

$$Zn_{(Cu\text{-}Zn)} = Zn^{2+} + 2e \qquad\qquad (3)$$

The heterogeneity of the formed corrosion products results in reduction of surface film protectivity and enhances the De-alloying process. As droplet holding time progresses the corrosion

products started to form and partially covered the brass surface leading to a decline in the corrosion rate as shown in the middle stage. Chloride ion penetrated through the precipitated heterogeneous zinc corrosion products and enhances the copper corrosion as:
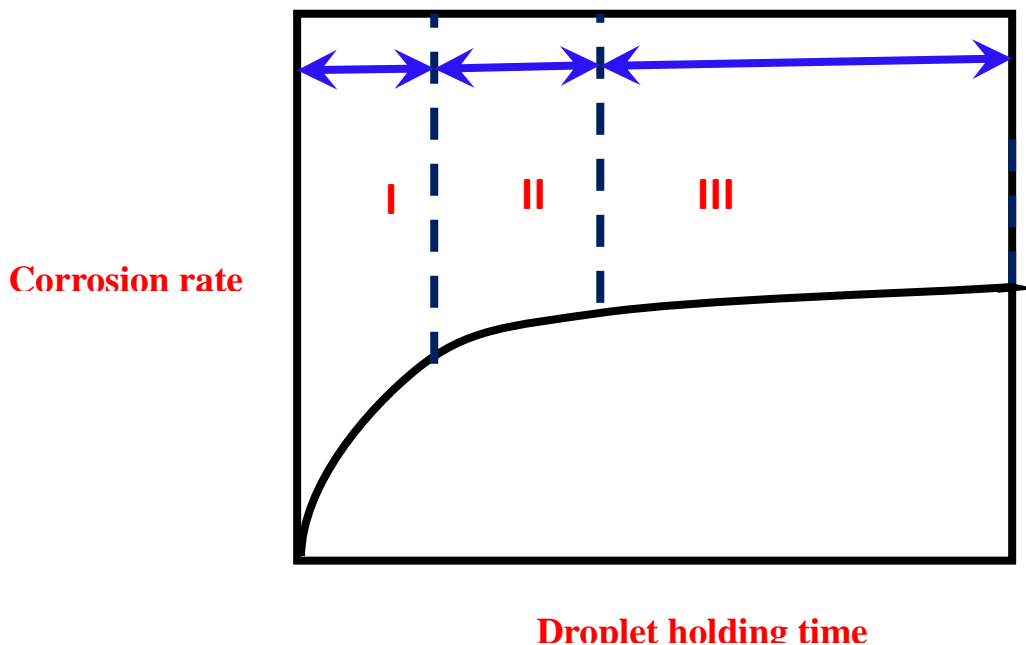
$$Cu_{(Cu-Zn)} = Cu^{2+} + 2e \qquad\qquad\qquad (4)$$

Figure 8. Mechanism of Brass corrosion within NaCl droplet

As the time progresses the droplet height decreases and the corrosion process is controlled by oxygen reduction process, which is enhanced during drying as a results of increasing the volume loss of NaCl electrolyte with time. The reduction process can described as:

$$O_2 + 4e + 2H_2O = 4OH^- \qquad\qquad\qquad (5)$$

The corrosion products of copper formed over the precipitated zinc corrosion products and caused a decrease in the corrosion rate during the last stage of monitoring. The observed steady state during the last stage of droplet holding time can be accounted to entire covering the surface with corrosion products. It can be concluded that double layer of corrosion products is formed and entirely covered the brass surface. The inner layer is rich in zinc corrosion products, while the outré layer is rich in copper corrosion products due to the initial rapid de-alloying of zinc [39]. It was reported previouslt that ZnO is also more soluble than Cu_2O in chloride media and hence dezincification is predicted [40]. The precipitation of zinc corrosion products as ZnO and $Zn_5(OH)_8Cl_2$ [41-43] as well as the copper corrosion products as Cu_2O and $Cu_2Cl(OH)_3$ [39, 44-45] leads eventually to entire covering the brass surface.

4. CONCLUSIONS

1- The corrosion rate decreases slowly during the initial stage of monitoring then eventually increases during the last stage of monitoring

2- The droplet height continually dropped during the evaporation process, while the volume loss increases as the droplet holding time increases.

3- The drop diameter remained relatively constant, while the contact angle continually decreased as droplet holding time progressed.

4- The corrosion rate decreases as the droplet height increases.

References

1. R.H. Heidersbach Jr., Ellis D. Verink Jr., *Corrosion* 28 (11) (1972) 397.
2. T.K.G. Namboodhiri, R.S. Chaudhary, B. Prakash, M.K. Agrawal, *Corros. Sci.* 22 (1982) 1037.
3. R.K. Dinnappa, S.M. Mayanna, *Corros. Sci.* 27 (1987) 349.
4. R.B. Rebak, J.R. Galvele, *Corros. Sci.* 29 (1989) 1003.
5. L. Burzynska, J. Stoch, Z. Zembura, *Solid State Ionics* 38 (1990) 179.
6. L. Burzynska, Z. Zembura, *Polish J. Chem.* 66 (1992) 503.
7. L. Burzynska, A. Maraszewska, Z. Zembura, *Corros. Sci.* 38 (1996) 337.
8. Z Avramovic, M. Antonijevic, *Corros. Sci.* 46 (2004) 2793–2802
9. V.K. Gouda, H.A. El-Sayed, S.M. Sayed, Proc. Int. Cong. Met. Corros., Maniz, vol. 8, 1981, p. 479.
10. A. Nagiub, F. Mansfeld, *Corros. Sci.* 43 (1987) 2147.
11. J. Morales, G.T. Fernandez, P. Esparza, S. Gonzalez, R.C. Salvarezza and A.J. Arvia, *Corros. Sci.* 37 (1995) 211.
12. J. Morales, G.T. Fernandez, S. Gonzalez, P. Esparza, R.C. Salvarezza and A.J. Arvia, *Corros. Sci.* 40 (1998) 177.
13. M. Kabasakaloglu, T. Kiyak, O. Sendil and A. Asan, *Applied Surf. Sci.* 193 (2002) 167.
14. J.Y. Zou, D.H. Wang and W.C. Qiu, *Electrochim. Acta* 42 (1997) 1733.
15. M. Fenelon, C.B. Breslin, *J. Appl. Electrochem.* 31 (2001) 509–516.
16. S. Mamas, T. Kiyak, M. Kabasakaloglu, A. Koc, *Mater. Chem. Phys.* 93 (2005) 41.
17. M. Osman, *Mater. Chem. Phys.* 71 (2001) 12.
18. V. Otieno-Alego, G.A. Hope, T. Notoya, D.P. Schweinsberg, *Corros. Sci.* 38 (1996) 213.
19. M. Kabasakaloǧlu, T. Kıyak, O. Sˌendil, A. Asan, *Appl. Surf. Sci.* 193 (2002) 167–174.
20. S.H. Sanad, H. Abbas, A.A. Ismail, K.M. El-Sobki, *Surf. Technol.* 25 (1985) 39.
21. S.L.F.A. de Costa, S.M.L. Agostinho, K. Nobe, *J. Electrochem. Soc.* 140 (1993) 3483.
22. A.K. Neufeld, I.S. Cole, A.M. Bond, S.A. Furman, *Corros. Sci.* 44 (2002) 555.
23. T.E. Graedel, *J. Electrochem. Soc.* 136 (1989) 193C.
24. N.D. Tomashov, *Corrosion* 20 (1964) 7.
25. G.A. El-Mahdy, *Corrosion* 59 (2003) 505.
26. M. Stratmann, H. Streckel, *Corros. Sci.* 30 (1990) 681.
27. M. Stratmann, H. Streckel, K.T. Kim, S. Crockett, *Corros. Sci.* (1990) 715.
28. T. Tsuru, K.-I. Tamiya, A. Nishikata, *Electrochim. Acta* 49 (2004) 2709.

29. A.K. Neufeld, L.S. Cole, A.M. Bond, S.A. Furman, *Corros. Sci.* 44 (2002) 555.
30. R.P. Cruz Vera, A. Nishikata, T. Tsuru, *Corros. Sci.* 38 (1996) 1397.
31. G.A. El-Mahdy, A. Nishikata, T. Tsuru, *Corros. Sci.* 42 (2000) 1509.
32. A. Nazarov, D. Thierry, *Electrochim. Acta* 49 (2004) 2717.
33. A. Nishikata, S. Kurnagai, T. Tsu, *Corr. Eng.* 43 (1994) 109.
34. A. Nishikata, T. Takahashi, B. Horu, T. Tsuri, *Corros. Eng.* 43 (1994) 225.
35. Q. Qu, C.i. Yan, Y. Wan, C. Cao, *Corros. Sci.* 44 (2002) 2789.
36. A.P. Yadav, A. Nishikata, T. Tsuru, *Corros. Sci*. 46 (2004) 361.
37. M. Stern, A.L. Geary, *J. Electrochem*. 104 (1957) 56.
38. G.A. El-Mahdy, A. Nishikata, T. Tsuru, *Corros. Sci.* 42 (2000) 183.
39. G.A.EL-Mahdy, *J. Appl. Electrochem*. 35 (2005)347.
40. O. Fruhwirth, G.W. Herzog and *J. Poulios, Surf. Technol*. 24 (1985) 293.
41. U. Bertocci, E.N. Pugh and R.E. Ricker, (edited by R. Gangloff and M. Ives) Environmentally-Induced Cracking of Metals, NACE, 1989, p. 273.
42. H.H. Rehan, N.A. Al-Moubarak and H.A. Al-Rafai, *Mater. Corros*. 52 (2001) 677.
43. L.G. Cox, *Ind. Eng. Chem*. 23 (1931) 902.
44. H.E. Johnson and J. Leja, *Corrosion* 22 (1966) 178.
45. C.J.E. Smith and A.N. Hughes, *Br. Corros. J.* 11 (1976) 12.